A search for non-$q\overline{q}$ mesons in the WA102 experiment at the CERN Omega Spectrometer

Presented by Andrew Kirk
representing
The WA102 collaboration
Annecy, Athens, Bergen, Birmingham, CERN, IHEP, IISN, JINR,
KEK, Miyazaki, Osaka, Oslo, Tohoku, Yamagata.

September 11, 1997

1 Introduction

The present understanding of strong interactions is that they are described by Quantum ChromoDynamics (QCD). This non-Abelian field theory not only describes how quarks and antiquarks interact, but also predicts that the gluons which are the quanta of the field will themselves interact to form mesons. If the object formed is composed entirely of valence gluons the meson is called a glueball, however if it is composed of a mixture of valence quarks, antiquarks and gluons (i.e. $q\overline{q}g$) it is called a hybrid. In addition, $q\overline{q}q\overline{q}$ states are also predicted.

The best estimate for the masses of glueballs comes from lattice gauge theory calculations [1] which show that the lightest glueball has $J^{PC} = 0^{++}$ and that

$$m(2^{++})/m(0^{++}) = 1.5$$

and depending on the extrapolation used from the lattice parameters to mass scale that

$$m(0^{++}) = (1500 - 1750)\text{MeV}.$$

The mass of the 0^{-+} glueball is predicted to be similar to that of the 2^{++} glueball whilst glueballs with other quantum numbers are predicted to be higher in mass.

The flux tube model has been used to calculate the masses of the lowest lying hybrid states and recent predictions [2] are that

$$m(1^{--}, 0^{-+}, 1^{-+}, 2^{-+}) \approx 1900 \text{ MeV}.$$

Hence, these non-$q\overline{q}$ states are predicted to be in the same mass range as the normal $q\overline{q}$ nonet members and hence we need a method of identifying them.

The following have been suggested as possible ways to identify gluonic states.

- To look for "oddballs": States with J^{PC} quantum numbers not allowed for normal $q\overline{q}$ states. For example $J^{PC} = 1^{-+}$.
- However the lightest non-$q\overline{q}$ states are predicted to have the same quantum numbers as $q\overline{q}$ states. Therefore we need to look for extra states, that is states that have quantum numbers of already completed nonets and that have masses which are sufficiently low that they are unlikely to be members of the radially excited nonets and hence they can not be described as being pure $q\overline{q}$ states.
- If extra states are found then in order to isolate which state is the likely non-$q\overline{q}$ state we can
  a) Look for states with unusual branching ratios.
  b) Look for states preferentially produced in gluon rich processes. These processes are described below.

Fig. 1 summarises several dynamical configurations which have been suggested as possible sources of gluonium and where experiments have been performed.

1. Pomeron-Pomeron scattering is shown in fig. 1a). The Pomeron is an object which can be described as a multi-gluon state, and is thought to be responsible for the large cross sections of diffractive reactions. Consequently Double Pomeron Exchange (DPE) is considered to be a possible source of glueballs.
2. The J/ψ decay is believed to be a highly glue rich channel either via the hadronic decay shown in fig. 1b), or via the radiative decay shown in fig. 1c).
3. Figure 1d) shows proton-antiproton annihilation; the annihilation region of quarks and antiquarks is a source of gluons where glueballs and hybrids could be produced.
4. Special hadronic reactions, an example of which is shown in fig. 1e) where the $\phi\phi$ system is thought to be produced via an intermediate state containing gluons. Reactions of this kind which have disconnected quark lines are said to be OZI violating [3].

The first reaction is the one studied by experiments WA76, WA91 and WA102 at the Omega spectrometer. In this paper the status of these experiments is reviewed, the possibility of a Glueball-$q\overline{q}$ filter in central production is discussed and this filter is then used in an analysis of the $K^0_S K^{\pm}\pi^{\mp}$ and $\pi^+\pi^-\pi^+\pi^-$ final states.

2 The Omega Central production experiments

There is considerable current interest in trying to isolate the lightest glueball. Several experiments have been performed using glue-rich production mechanisms. One such mechanism is

Double Pomeron Exchange (DPE) where the Pomeron is thought to be a multi-gluonic object. Consequently it has been anticipated that production of glueballs may be especially favoured in this process [4].

The Omega central production experiments (WA76, WA91 and WA102) are designed to study exclusive final states formed in the reaction

$$\mathrm{pp} \longrightarrow \mathrm{p}_f X^0 \mathrm{p}_s,$$

where the subscripts f and s refer to the fastest and slowest particles in the laboratory frame respectively and X^0 represents the central system. Such reactions are expected to be mediated by double exchange processes where both Pomeron and Reggeon exchange can occur.

The layout of the 1994 run of WA91 is shown in fig. 2. The positively charged H1 beam in the West Area was incident on a 60 cm long hydrogen target. A set of ten 20 μm pitch μ-strip detectors were used to perform an accurate measurement of the incident beam's trajectory. The outgoing fast track, which had a momentum in the range 300 to 450 GeV/c, was measured by two sets of 4 μ-strip detectors placed 8 and 12 m downstream from the target. The standard Ω MWPC's and Drift Chambers were used to measure the medium momentum tracks ($\approx$ 1 to 40 GeV/c) leaving the interaction region, with particle identification coming from two threshold Cerenkov counters C1 and C2. Photon detection was provided by the GAMS-4000 and OLGA lead glass calorimeters.

The trigger was designed to enhance double exchange processes with respect to single exchange and elastic processes. Details of the trigger conditions, the data processing and event selection have been given in previous publications [5]. A summary of that data taking history of the experiments is given in table 1. As can be seen experiment WA102 collected 500 million events which is a factor of 50 larger than the original WA76 experiment. This large increase in statistics enables an in depth study of the observed resonances as a function of kinematical variables the results of which are described below.

3 The possibility of a Glueball-$q\overline{q}$ filter in central production

The experiments have been performed at incident beam momenta of 85, 300 and 450 GeV/c, corresponding to centre-of-mass energies of $\sqrt{s}$ = 12.7, 23.8 and 28 GeV. Theoretical predictions [6] of the evolution of the different exchange mechanisms with centre of mass energy, $\sqrt{s}$, suggest that

$$\begin{aligned} \sigma(\mathrm{RR}) &\sim s^{-1}, \\ \sigma(\mathrm{RP}) &\sim s^{-0.5}, \\ \sigma(\mathrm{PP}) &\sim \text{constant}, \end{aligned}$$

where RR, RP and PP refer to Reggeon-Reggeon, Reggeon-Pomeron and Pomeron-Pomeron exchange respectively. Hence we expect Double Pomeron Exchange (DPE) to be more significant at high energies, whereas the Reggeon-Reggeon and Reggeon-Pomeron mechanisms will

be of decreasing importance. The decrease of the non-DPE cross section with energy can be inferred from data taken by the WA76 collaboration using pp interactions at $\sqrt{s}$ of 12.7 GeV and 23.8 GeV [7]. The $\pi^+\pi^-$ mass spectra for the two cases show that the signal-to-background ratio for the $\rho^0(770)$ is much lower at high energy, and the WA76 collaboration report that the ratio of the $\rho^0(770)$ cross sections at 23.8 GeV and 12.7 GeV is 0.44 ± 0.07. Since isospin 1 states such as the $\rho^0(770)$ cannot be produced by DPE, the decrease of the $\rho^0(770)$ signal at high $\sqrt{s}$ is consistent with DPE becoming relatively more important with increasing energy with respect to other exchange processes.

However, even in the case of pure DPE the exchanged particles still have to couple to a final state meson. The coupling of the two exchanged particles can either be by gluon exchange or quark exchange. Assuming the Pomeron is a colour singlet gluonic system if a gluon is exchanged then a gluonic state is produced, whereas if a quark is exchanged then a $q\overline{q}$ state is produced (see figures 3a) and b) respectively). It has been suggested recently [8] that for small differences in transverse momentum between the two exchanged particles an enhancement in the production of glueballs relative to $q\overline{q}$ states may occur.

Recently the WA91 collaboration has published a paper [9] showing that the observed centrally produced resonances depend on the angle between the outgoing slow and fast protons. In order to describe the data in terms of a physical model, Close and Kirk [8] have proposed that the data be analysed in terms of the difference in transverse momentum between the particles exchanged from the fast and slow vertices.

The trigger is described in detail in ref. [9]. In brief, the trigger separates the data into two categories. One where the slow and fast particles are on the same side of the beam, *i.e.* a small azimuthal angle between the outgoing protons (classified as LL) and one where the slow and fast particles are on the opposite side of the beam, *i.e.* the azimuthal angle between the outgoing protons is near to 180 degrees, (classified as LR).

In ref. [9] it was shown that the centrally produced resonances depended on the trigger type i.e. the resonances observed in the LL trigger were different to those observed in the LR trigger. This difference was not due to any acceptance or trigger bias but appeared to be related to the angle between the outgoing protons. Figures 3c) and d) show schematic representations of the LL and LR triggers respectively in the centre of mass of the beam plus target where the longitudinal (x) axis is defined to be along the beam direction. In the case of the LL trigger (figure 3c)) the transverse momentum vector of each exchanged particle has the same sign whereas for the LR trigger (figure 3d)) they have the opposite sign. Hence the difference in the transverse momentum vectors of the two exchanged particles is greater in the LR trigger than in the LL trigger. The difference in the transverse momentum vectors (dP_T) is defined to be

$$dP_T = \sqrt{(P_{y1} - P_{y2})^2 + (P_{z1} - P_{z2})^2}$$

where Py_i, Pz_i are the y and z components of the momentum of the ith exchanged particle in the pp centre of mass system.

Figures 4a) and b) show the dP_T spectrum for the LL and LR trigger types respectively. As can be seen the LL trigger type have access to events with smaller dP_T. It has been shown by Monte Carlo simulation that this effect is not due to the fact that the LR events have additional

trigger requirements but it is due only to the fact that the two protons recoil on the same (LL) or opposite (LR) side of the beam direction [9].

The effect that different cuts in dP_T have on the $\pi^+\pi^-$ mass spectrum are shown in figures 4c), d) and e). As can be seen, for $dP_T < 0.2$ GeV there is effectively no $\rho^0(770)$ or $f_2(1270)$ signals. These signals only become apparent as dP_T increases. However the $f_0(980)$, which is responsible for the sharp drop in the spectrum around 1 GeV, is clearly visible in the small dP_T sample.

Figures 5a), b) and c) show the effect of the dP_T cut on the K^+K^- mass spectrum where structures can be observed in the 1.5 and 1.7 GeV mass region which have been previously identified as the $f_2'(1525)$ and the $f_J(1710)$ [10]. As can be seen, the $f_2'(1525)$ is produced dominantly at high dP_T, whereas the $f_J(1710)$ is produced dominantly at low dP_T.

In the $\pi^+\pi^-\pi^+\pi^-$ mass spectrum a dramatic effect is observed, see figures 5d), e) and f). The $f_1(1285)$ signal has virtually disappeared at low dP_T whereas the $f_0(1500)$ and $f_2(1930)$ signals remain.

Figure 6 shows a similar effect in the $K_S^0K^\pm\pi^\mp$ and $\eta\pi^+\pi^-$ channels where the $f_1(1285)$, $f_1(1420)$ and η' are all more prominent in the large dP_T sample and start to disappear at low dP_T.

In fact it has been observed that all the undisputed $q\overline{q}$ states (i.e. $\rho^0(770)$, η', $f_2(1270)$, $f_1(1285)$, $f_2'(1525)$ etc.) are suppressed as dP_T goes to zero, whereas the glueball candidates $f_J(1710)$, $f_0(1500)$ and $f_2(1930)$ survive. It is also interesting to note that the enigmatic $f_0(980)$, a possible non-$q\overline{q}$ meson or $K\overline{K}$ molecule state does not behave as a normal $q\overline{q}$ state.

A Monte Carlo simulation of the trigger, detector acceptances and reconstruction program shows that there is very little difference in the acceptance as a function of dP_T in the different mass intervals considered within a given channel and hence the observed differences in resonance production can not be explained as acceptance effects.

It has previously been observed that the resonances produced in the central region depend on the four momentum transferred from the fast (t_f) and slow vertices (t_s) [7]. The $\pi^+\pi^-$ mass spectrum is shown for the case where $|t_f|$ and $|t_s|$ are both less than 0.15 GeV^2 in figure 7a) and in figure 7b) for the case when $|t_f|$ and $|t_s|$ are both greater than 0.15 GeV^2. As can be seen the amount of $\rho^0(770)$ and $f_2(1270)$ does change as a function of this cut. In figures 7c) and d) the dP_T distribution for these two cases is shown. As can be seen the events that have small $|t|$ are restricted to small values of dP_T. To show that dP_T is the most important underlying dynamical effect the dP_T cut has been applied to the sample of events with large $|t|$. Figures 7e), f) and g) show the events when $|t_f|$ and $|t_s|$ are both greater than 0.15 GeV^2 for $dP_T \leq 0.2$ GeV, $0.2 \leq dP_T \leq 0.5$ GeV and $dP_T \geq 0.5$ GeV respectively. As can be seen the dP_T cut still works in this sample.

In summary, the undisputed $q\overline{q}$ states are observed to be suppressed at small dP_T, but the glueball candidates $f_0(1500)$, $f_J(1710)$, and $f_2(1930)$ survive. In order to investigate this effect further a more complete analysis of the $\pi^+\pi^-\pi^+\pi^-$ and $K_S^0K^\pm\pi^\mp$ channels is presented below.

4 Results on $pp \to p_f(\pi^+\pi^-\pi^+\pi^-)p_s$

The WA76 and WA91 collaborations have studied the centrally produced $\pi^+\pi^-\pi^+\pi^-$ final state in the reaction

$$pp \to p_f(\pi^+\pi^-\pi^+\pi^-)p_s \quad (1)$$

at 85 [11], 300 [12], and 450 GeV/c [13]. The subscripts f and s indicate the fastest and slowest particles in the laboratory respectively. In addition to the $f_1(1285)$, which was observed at all energies, the WA76 collaboration observed two new states at 1.45 and 1.9 GeV in their 300 GeV/c data [12]. In contrast, no clear evidence was seen for these states in the 85 GeV/c data of the same experiment [11]. The increase in cross section with increased incident energy [12] is consistent with the formation of these states via a double Pomeron exchange mechanism, which is predicted to be a source of gluonic states [4].

The WA91 experiment [13], which studied reaction (1) at 450 GeV/c, confirmed the existence of these states and, from a spin analysis, showed that the peak at 1.45 GeV had $I^GJ^{PC} = 0^+0^{++}$ and that the peak at 1.9 GeV had $I^GJ^{PC} = 0^+2^{++}$; hence they were called the $f_0(1450)$ and $f_2(1900)$ respectively. In a reanalysis of this data [14], the WA91 collaboration showed that it was possible to describe the $f_0(1450)$ as being due to the interference between the $f_0(1300)$ and the $f_0(1500)$.

A spin-parity analysis of the $\pi^+\pi^-\pi^+\pi^-$ channel has been performed using an isobar model [13]. The results of the best fit are shown in fig. 8 for the total data sample and in fig. 9 for three ranges of dP_T. The $f_1(1285)$ is clearly seen in the $J^P = 1^+$ $\rho\rho$. Superimposed on the $J^P = 1^+$ $\rho\rho$ wave for the total sample is the Breit Wigner convoluted with a Gaussian used to describe the $f_1(1285)$ in the fit to the mass spectrum. As can be seen the $f_1(1285)$ is well represented in both size and shape. From fig. 9 it can be seen that the $f_1(1285)$ dies away for $dP_T \leq 0.2$ GeV.

The $J^P = 0^+\rho\rho$ distribution in fig. 8 shows a peak at 1.45 GeV together with a broad enhancement around 2 GeV. From fig. 9 it can be seen that the peak in the $J^P = 0^+\rho\rho$ wave around 1.45 GeV remains for $dP_T \leq 0.2$ GeV while the $J^P = 0^+$ enhancement at 2.0 GeV becomes less important: which shows that the dP_T effect is not simply a J^P filter.

A fit has first been performed to the total $J^P = 0^+\rho\rho$ distribution in fig. 8 using a K matrix formalism [15] including poles to describe the interference between the $f_0(1300)$, the $f_0(1500)$ and a possible state at 2 GeV. The result of the fit is superimposed on the $J^P = 0^+\rho\rho$ distribution shown in fig. 8 and well describes the data. The resulting resonance parameters for the $f_0(1300)$ and $f_0(1500)$ are very similar to those found by Crystal Barrel [16].

As can be seen from fig. 8 neither the $J^P = 2^+$ $a_2(1320)\pi$ nor the $J^P = 2^+$ $f_2(1270)(\pi\pi)_{Swave}$ alone can describe the $f_2(1900)$ peak observed in the mass spectrum. However, the sum of the two waves accounts for most of the $f_2(1900)$ signal. The $a_2(1320)\pi$ distribution and the $f_2(1270)(\pi\pi)_{Swave}$ distribution peak at different masses which suggests that the $f_2(1900)$ could be composed of two $J^{PC} = 2^{++}$ resonances but neither distribution is well represented by a Breit-Wigner. However, the sum of the $J^P = 2^+$ $a_2(1320)\pi$ and $J^P = 2^+$ $f_2(1270)(\pi\pi)_{Swave}$ waves has been fitted with a single Breit-Wigner, giving a better description, with M = 1960 $\pm$ 30 MeV and Γ = 460 $\pm$ 40 MeV. These values are compatible with those coming from the fit to the total mass spectrum.

In addition to these waves, a $J^P = 2^-$ $a_2(1320)\pi$ wave was required in the fit. The resulting $J^P = 2^-$ $a_2(1320)\pi$ wave is shown in fig. 8 where a broad enhancement is observed which peaks at 1.6 GeV. Other experiments have observed evidence for $J^{PC} = 2^{-+}$ states in this region. In the reaction $\gamma\gamma \to \eta\pi\pi$ the Crystal Ball collaboration [17] reported a $J^{PC} = 2^{-+}$ state decaying to $a_2(1320)\pi$ and $a_0(980)\pi$ with a mass of $1881 \pm 32 \pm 40$ MeV and a width of $221 \pm 92 \pm 44$ MeV. In $p\overline{p}$ interactions the Crystal Barrel collaboration [18] reported the observation of two $J^{PC} = 2^{-+}$ states in the $\eta\pi\pi$ final state. The first state, called the $\eta_2(1620)$, had a mass of $1645 \pm 14 \pm 5$ MeV and a width of $180 \pm 40 \pm 25$ MeV and the second state, called the $\eta_2(1875)$, had a mass of $1875 \pm 20 \pm 35$ MeV and a width of $250 \pm 25 \pm 45$ MeV.

As can be seen from fig. 8 the $J^P = 2^-$ $a_2(1320)\pi$ wave observed in this experiment is consistent with the two η_2 resonances discussed above with both states decaying to $a_2(1320)\pi$.

As is observed from figs. 5d) and 9 the $f_1(1285)$ signal almost disappears at small dP_T. In addition, the $2^{-+}a_2(1320)\pi$ signal is also suppressed at small dP_T. This behaviour is consistent with the signals being due to standard $q\overline{q}$ states [8].

The $0^{++}\rho\rho$ wave shows that the peak at 1.45 GeV is still prominent at small dP_T. If the peak is interpreted as the interference between the $f_0(1300)$ and $f_0(1500)$ then both must have a similar dP_T dependence. The broad peak at 2.0 GeV in the $0^{++}\rho\rho$ wave, called the $f_0(2000)$, is less prominent at small dP_T and is more consistent with other $q\overline{q}$ states.

As can be seen from figure 9 at small dP_T the $f_2(1900)$ signal is still important. This is the first evidence of a non-zero spin resonance produced at small dP_T and hence shows that the dP_T effect is not just a $J^P = 0^+$ filter.

In summary, in the centrally produced $\pi^+\pi^-\pi^+\pi^-$ mass spectrum two interesting structures are observed at 1.45 and 1.9 GeV. A spin analysis shows that the underlying resonance structure is more complex. The peak at 1.45 GeV is found to have $J^{PC} = 0^{++}$ and to decay to $\rho\rho$; it can be interpreted as an interference between the $f_0(1300)$ and $f_0(1500)$. The peak observed at 1.9 GeV appears as a broad enhancement in the mass spectrum and is found to decay to $a_2(1320)\pi$ and $f_2(1270)\pi\pi$ with $J^{PC} = 2^{++}$. Confirmation is found for two $J^{PC} = 2^{-+}$ resonances, called the $\eta_2(1620)$ and $\eta_2(1875)$ decaying to $a_2(1320)\pi$. There is also evidence for a broad state with $J^{PC} = 0^{++}$ decaying to $\rho\rho$, called the $f_0(2000)$.

5 Results on $pp \to p_f(K\overline{K}\pi)p_s$

In previous analyses [19, 20, 21] of the centrally produced $K^0_S K^\pm \pi^\mp$ system the peaks observed at 1.28 and 1.42 GeV were found to have $J^{PG} = 1^{++}$ and hence were identified with the $f_1(1285)$ and $f_1(1420)$ respectively. However, due to the limited statistics a 10% 0^{-+} contribution could not be excluded [21].

Originally the $f_1(1420)$ was thought to be the $s\overline{s}$ isoscalar member of the ground state 1^{++} nonet, the other members being the $a_1(1260)$ triplet, the $K_1(1270/1400)$ and the $f_1(1285)$. The $f_1(1420)$ was found to decay dominantly to $K^*\overline{K}$ hence reinforcing its $s\overline{s}$ assignment. It is commonly accepted that $s\overline{s}$ objects should be preferentially produced in K^- incident experiments whereas in the study of the reaction

$$K^- p \to K^0_S K^\pm \pi^\mp \Lambda$$

two experiments [22, 23] observed only weak evidence for a $f_1(1420)$ signal. Instead they found evidence for a new $J^{PC} = 1^{++}$ state with a mass of 1.53 GeV and a width of 100 MeV, called the D$'/f_1(1510)$. It was suggested that this state is a better candidate for the $s\overline{s}$ member of the 1^{++} nonet based on its production.

Therefore, the 1^{++} nonet appears to have ten candidates with the $f_1(1420)$ thought to be the extra state. As a 1^{++} state its mass is considered to be too low to be a glueball or hybrid state, and it has been suggested that it could be either a hybrid [24], a four quark state [25] or a $K^*\overline{K}$ molecule [26, 27].

A study of the centrally produced exclusive final states formed in the reactions

$$pp \to p_f(K^0_S K^\pm \pi^\mp) p_s \tag{2}$$

and

$$pp \to p_f(K^0_S K^0_S \pi^0) p_s \tag{3}$$

at 450 GeV/c has been performed.

Fig. 10a) shows the $K^0_S K^\pm \pi^\mp$ effective mass spectrum where the kaon has been positively identified by the Čerenkov counter (5 647 events). A Dalitz plot analysis of the $K^0_S K^\pm \pi^\mp$ final state has been performed using Zemach tensors and a standard isobar model [28]. The fit shows that the $J^{PG} = 1^{++}$ $a_0(980)\pi$ wave is the only wave required to describe the $f_1(1285)$ peak and that the $J^{PG} = 1^{++}$ $K^*\overline{K}$ wave is the only wave required to describe the $f_1(1420)$ peak. The addition of 0^{-+} or any other waves up to J equals 2 does not increase the likelihood significantly. The results of the fit are shown in fig.10 b),c) and d). It is interesting to note that there is no evidence for the $f_1(1510)$.

In addition, a $J^{PG} = 2^{-+}$ $K^*\overline{K}$ wave is found to be required in the 1.6 GeV region as shown in fig 10e). Superimposed on fig 10e) is the Breit-Wigner found to describe the $\eta_2(1620)$ decaying to $a_2(1320)\pi$ in the analysis of the $\pi^+\pi^-\pi^+\pi^-$ final state of this experiment. As can be seen the $J^{PG} = 2^{-+}$ $K^*\overline{K}$ wave is consistent with this in mass and width.

From a Dalitz plot analysis of the $K^0_S K^\pm \pi^\mp$ system only the J^{PG} of the final state can be determined. In order to determine the C parity, and hence the isospin of the final states, a study of the $K^0_S K^0_S \pi^0$ system is required since only C parity positive states can be observed in this channel.

Fig. 11a) shows the $K^0_S K^0_S \pi^0$ effective mass spectrum (949 events) where clear peaks at 1.28 and 1.42 GeV can be seen. A spin analysis has been performed on this sample and shows that the peaks at 1.28 and 1.42 GeV have $J^{PC} = 1^{++}$. The small number of events does not allow a statistically significant signal in the $J^{PC} = 2^{-+}$ wave to be extracted.

Therefore, we have clearly identified both the $f_1(1285)$ and the $f_1(1420)$ to have $I^G J^{PC} = 0^+1^{++}$. The $f_1(1285)$ is found to decay only to $a_0(980)\pi$ while the $f_1(1420)$ is found to decay only to $K^*\overline{K}$. There is also evidence for a $J^{PG} = 2^{-+}$ $K^*\overline{K}$ signal consistent with the $\eta_2(1620)$.

The $f_1(1285)$ has also been observed in the $\pi^+\pi^-\pi^+\pi^-$ channel of this experiment [30] and its branching ratio to $K\overline{K}\pi$ and 4π has been calculated taking into account the unseen decay

modes and gives

$$\frac{f_1(1285) \to K\overline{K}\pi}{f_1(1285) \to 4\pi} = 0.265 \pm 0.01 \pm 0.01. \quad (4)$$

This is a considerable improvement in accuracy on our previous determination [31].

Assuming the signal in the $J^{PC} = 2^{-+}$ $K^*\overline{K}$ wave to be due to the $\eta_2(1620)$ observed decaying to $a_2(1320)\pi$ in the $\pi^+\pi^-\pi^+\pi^-$ channel [30] the branching ratio for the $\eta_2(1620)$ to $K\overline{K}\pi$ and $a_2(1320)\pi$ has been calculated taking into account the unseen decay modes and gives

$$\frac{\eta_2(1620) \to K\overline{K}\pi}{\eta_2(1620) \to a_2(1320)\pi} = 0.07 \pm 0.02 \pm 0.02. \quad (5)$$

Since no signal is observed for the $f_1(1510)$ in the 1^{++} $K^*\overline{K}$ wave, an upper limit for its production in central collisions relative to the $f_1(1420)$ has been calculated and gives

$$\frac{f_1(1510) \to K^*\overline{K}}{f_1(1420) \to K^*\overline{K}} < 0.03 \qquad at\ 90\%\ CL. \quad (6)$$

A study of the $K^0_S K^\pm \pi^\mp$ mass spectrum as a function of dP_T is presented in fig. 6a), b) and c) for $dP_T \leq 0.2$ GeV, $0.2 \leq dP_T \leq 0.5$ GeV and $dP_T \geq 0.5$ GeV respectively. As can be seen both the $f_1(1285)$ and $f_1(1420)$ signals behave similarly, which is consistent with both states having the same underlying dynamical structure.

In summary, clear $f_1(1285)$ and $f_1(1420)$ signals are observed. A spin parity analysis shows that both are $I^G J^{PC} = 0^+1^{++}$ states. The $f_1(1285)$ is found to decay via $a_0(980)\pi$ while the $f_1(1420)$ is found to decay only to $K^*\overline{K}$; no 0^{-+} or 1^{+-} waves are required to describe the data. The dP_T dependence of both states is similar and is consistent with both states having a $q\overline{q}$ nature. There is also evidence for a $K^*\overline{K}$ decay mode of the $\eta_2(1620)$.

6 Summary of the effects of the dP_T filter

In order to calculate the contribution of each resonance as a function of the dP_T the mass spectra have been fitted with the parameters of the resonances fixed to those obtained from the fits to the total data. The results of these fits are summarised in figure 12 where the percentage of each resonance as a function of dP_T is presented. Figure 13 shows the ratio of the number of events for $dP_T < 0.2$ GeV to the number of events for $dP_T > 0.5$ GeV for each resonance considered. As can be seen all the undisputed $q\overline{q}$ states have a small value for this ratio whereas the interesting states have a high value.

7 Conclusions

Preliminary results indicate the possibility of a glueball-$q\overline{q}$ filter mechanism in central production. All the undisputed $q\overline{q}$ states are observed to be suppressed at small dP_T, but the glueball candidates $f_0(1500)$, $f_J(1710)$, and $f_2(1930)$, together with the enigmatic $f_0(980)$, survive.

Experiment WA102 collected 500 million events during 1995 and 1996 and hence we have a large amount of data in many other channels to analyse. After the analysis of more channels we hope to be able to understand more fully the nature of this potentially very promising kinematical filter.

References

[1] G. Bali et al. (UKQCD), Phys. Lett. **B309** (1993) 378;

D. Weingarten, hep-lat/9608070;

J. Sexton et al., Phys. Rev. Lett. **75** (1995) 4563;

F.E. Close and M.J. Teper, "On the lightest Scalar Glueball" Rutherford Appleton Laboratory report no. RAL-96-040; Oxford University report no. OUTP-96-35P

[2] N. Isgur, AIP. Conf. Proc. 185, Particles and Fields 36, Glueballs, hybrids and exotic hadrons, (1988) 3

[3] S. Okuba, Phys. Lett. **5** (1963) 165;
G. Zweig, CERN/TH 401,402,412 (1964);
J. Iizuka, Prog. Theor. Phys. Suppl. **37-38** (1966) 21.

[4] D.Robson, Nucl Phys **B130** (1977) 328;
F.E. Close, Rep. Prog. Phys. **51** (1988) 833.

[5] T.A. Armstrong *et al.,* Nucl. Instr. and Methods **A274** (1989) 165;
F. Antinori *et al.,* Il Nuovo Cimento **A107** (1994) 1857.

[6] S.N. Ganguli and D.P. Roy, Phys. Rep. **67** (1980) 203.

[7] T.A. Armstrong et al., Zeit. Phys. **C 51** (1991) 351.

[8] F.E. Close and A. Kirk, Phys. Lett. **B397** (1997) 333.

[9] D. Barberis et al., Phys. Lett. **B 388** (1996) 853.

[10] T.A. Armstrong et al., Phys. Lett. **B 227** (1989) 186.

[11] T. A. Armstrong *et al.,* Zeit. Phys. **C43** (1989) 55.

[12] T. A. Armstrong *et al.,* Phys. Lett. **B228** (1989) 536.

[13] S. Abatzis *et al.,* Phys. Lett. **B324** (1994) 509.

[14] F. Antinori *et al.,* Phys. Lett. **B353** (1995) 589.

[15] S.U. Chung *et al.,* Ann. d. Physik. **4** (1995) 404.

[16] A. Abele *et al.,* Nucl. Phys. **A609** (1996) 562.

[17] H. Karch *et al.,* Zeit. Phys. **C54** (1992) 33.

[18] C. Amsler *et al.,* Zeit. Phys. **C71** (1996) 227.

[19] T. Armstrong *et al.*, Phys. Lett. **B146** (1984) 273;
T. Armstrong *et al.*, Z. Phys. **C34** (1987) 23.

[20] T. Armstrong *et al.*, Phys. Lett. **B221** (1989) 216.

[21] T. Armstrong *et al.*, Z. Phys. **C56** (1992) 29.

[22] Ph. Gavillet *et al.*, Z.Phys **C16** (1982) 119.

[23] D. Aston *et al.*, Phys. Lett. **B201** (1988) 573.

[24] S. Ishida *et al.*, Prog. Theor. Phys. **82** (1989) 119.

[25] F.E. Close, Rutherford preprint RAL-87-072. D. Caldwell, Mod. Phys. Lett. **A2** (1987) 771.

[26] J. Weinstein, AIP. Conf. Proc. 185, Particles and Fields 36, Glueballs, hybrids and exotic hadrons, (1988) 400.

[27] R.S. Longacre Phys. Rev **D42** (1990) 874.

[28] Ch. Zemach, Phys. Rev. **B133** (1964) 1201;
C. Dionisi *et al.*, Nucl. Phys. **B169** (1980) 1.

[29] S.M. Flatté, Phys. Lett. **B63** (1976) 224.

[30] D. Barberis *et al.,* CERN-PPE/97-89, hep-ex/9707021, Submitted to Phys. Lett.

[31] T. Armstrong *et al.,* Phys. Lett. **B228** (1989) 536.

Tables

Table 1: Data taking summary.

Year	Expt	Momentum GeV/c	Beam	$\sqrt{s}$ GeV	Particle I.D.	Triggers 10^6
1982	WA76	85	π^+/p	12.7	$\pi/K/p$	10
1986	WA76′	300	p	23.8	$\pi/K/p + \gamma$	12
1991	WA91 Test	450	p	29	γ	3
1992	WA91	450	p	29	γ	40
1994	WA91	450	p	29	$\pi/K/p + \gamma$	40
1995	WA102	450	p	29	γ	200
1996	WA102	450	p	29	$\pi/K/p + \gamma$	300

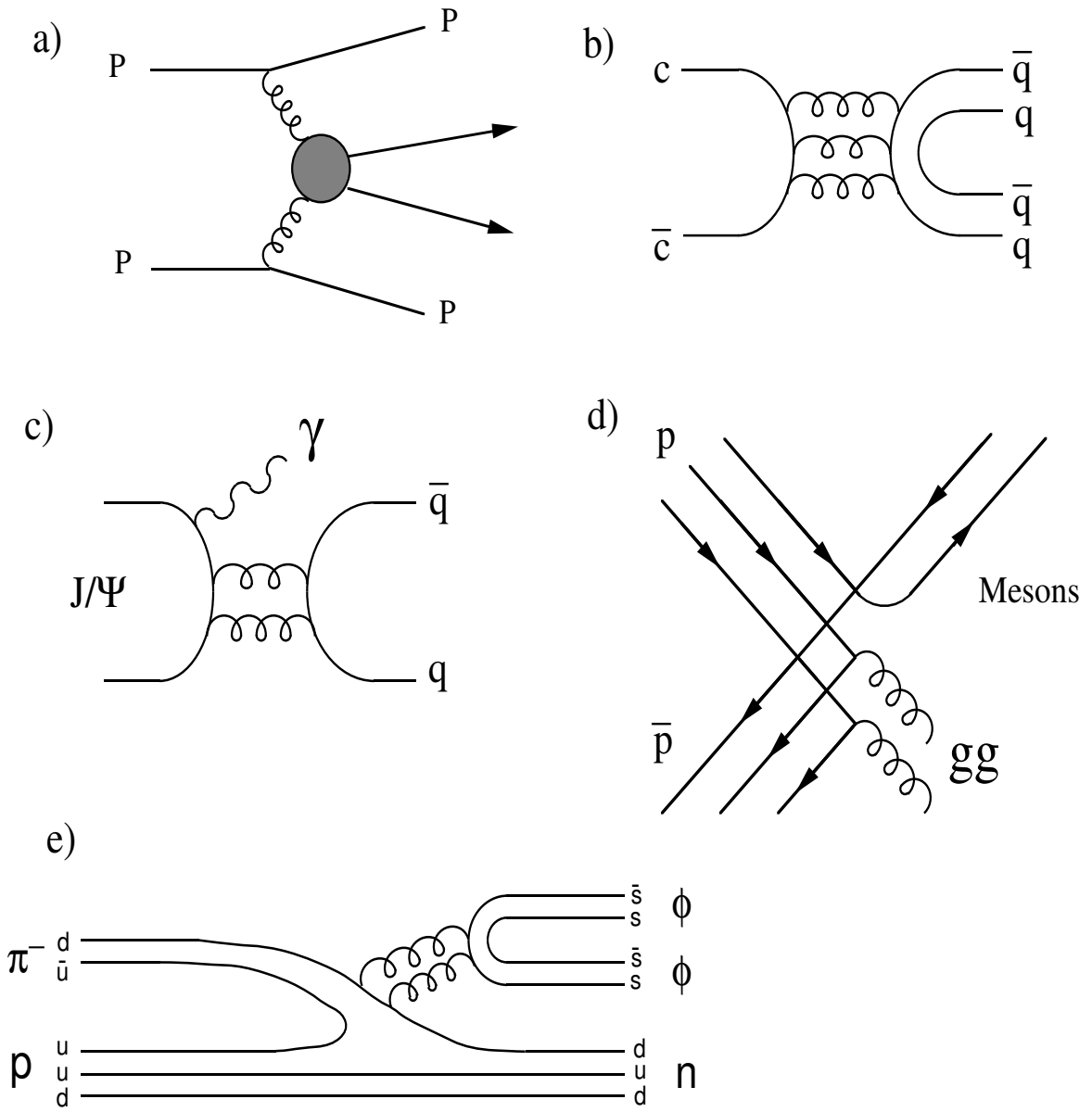

Figure 1: Gluon rich channels. Dynamical configurations that have been used to study light hadron spectroscopy in a search for glueball states.

Figure 2: Layout of the Ω spectrometer for WA91.

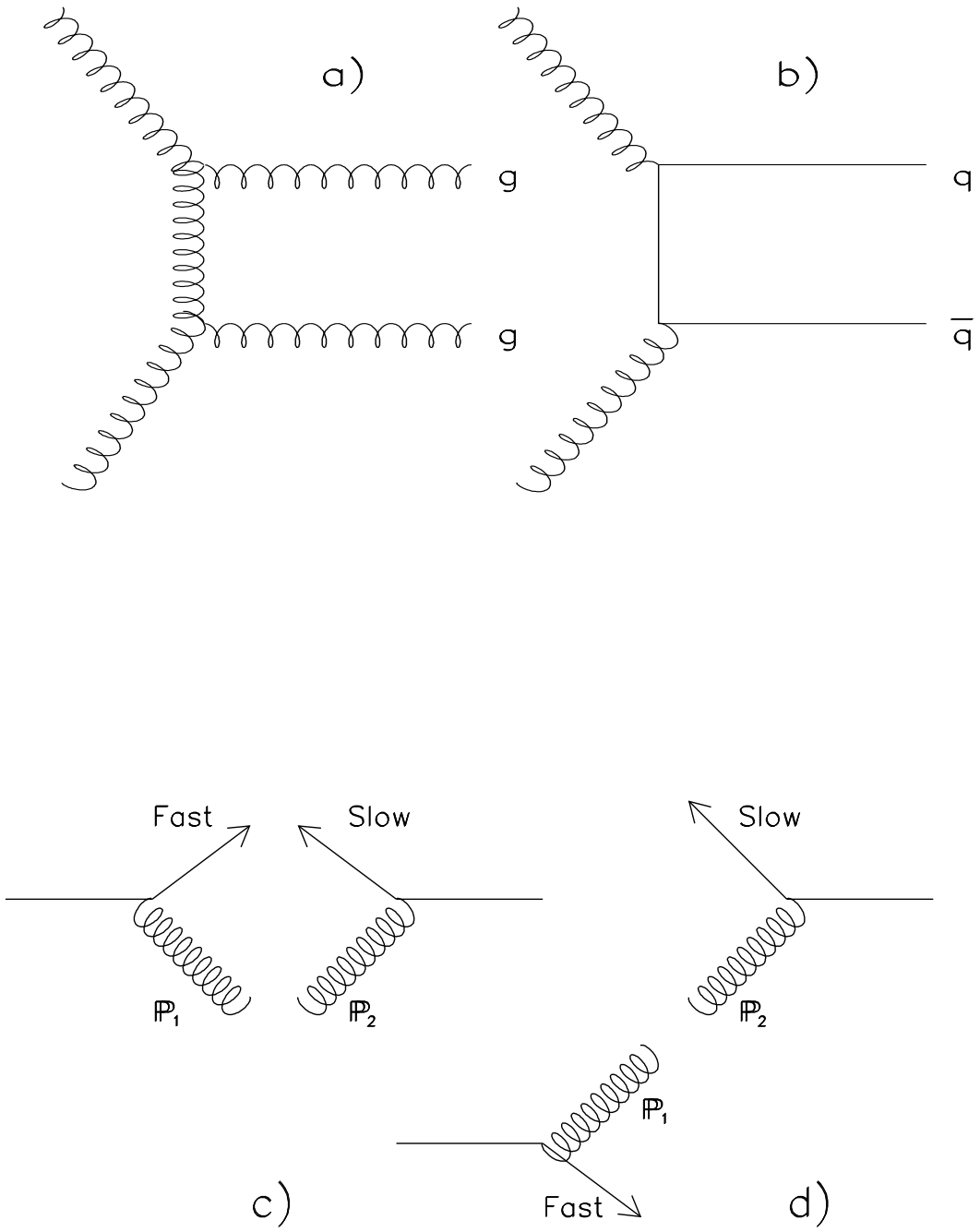

Figure 3: Schematic diagrams of the coupling of the exchange particles into the final state meson for a) gluon exchange and b) quark exchange. Schematic diagrams in the CM for c) LL and d) LR triggers.

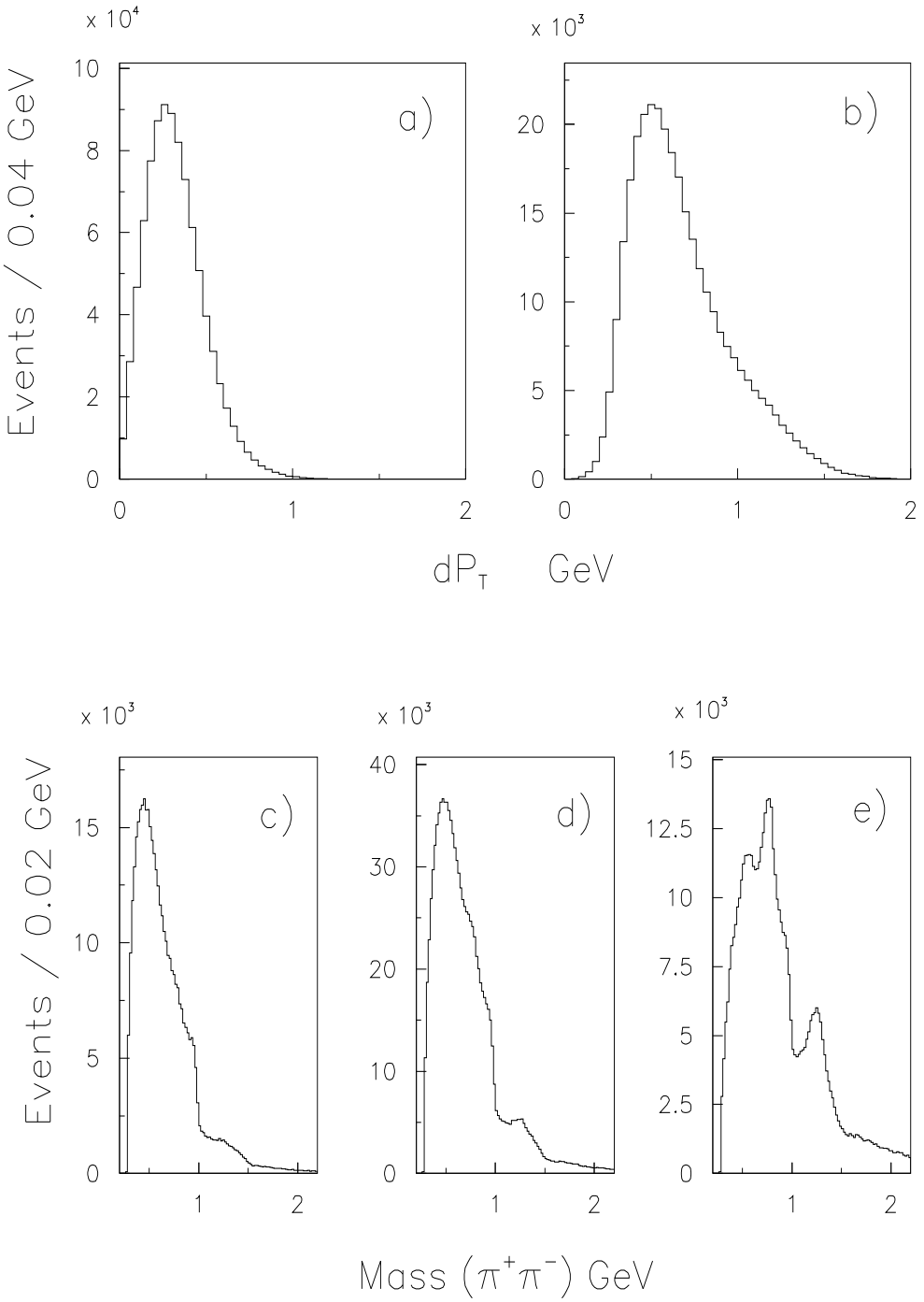

Figure 4: dP_T for a) LL and b) LR triggered events. The $\pi^+\pi^-$ mass spectrum for c) $dP_T < 0.2$ GeV, d) $0.2 < dP_T < 0.5$ GeV and e) $dP_T > 0.5$ GeV.

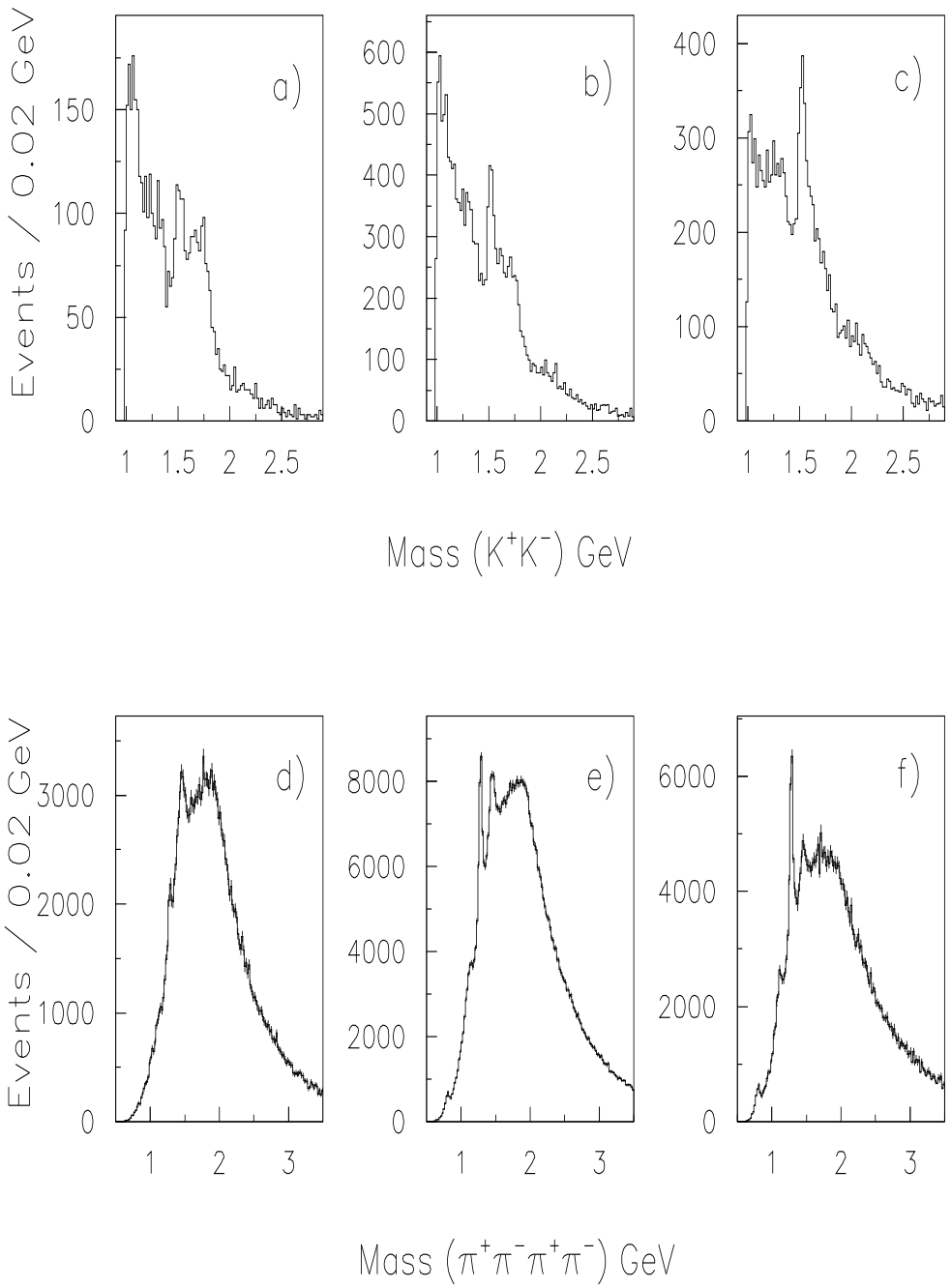

Figure 5: K^+K^- mass spectrum for a) $dP_T < 0.2$ GeV, b) $0.2 < dP_T < 0.5$ GeV and c) $dP_T > 0.5$ GeV and the $\pi^+\pi^-\pi^+\pi^-$ mass spectrum for d) $dP_T < 0.2$ GeV, e) $0.2 < dP_T < 0.5$ GeV and f) $dP_T > 0.5$ GeV.

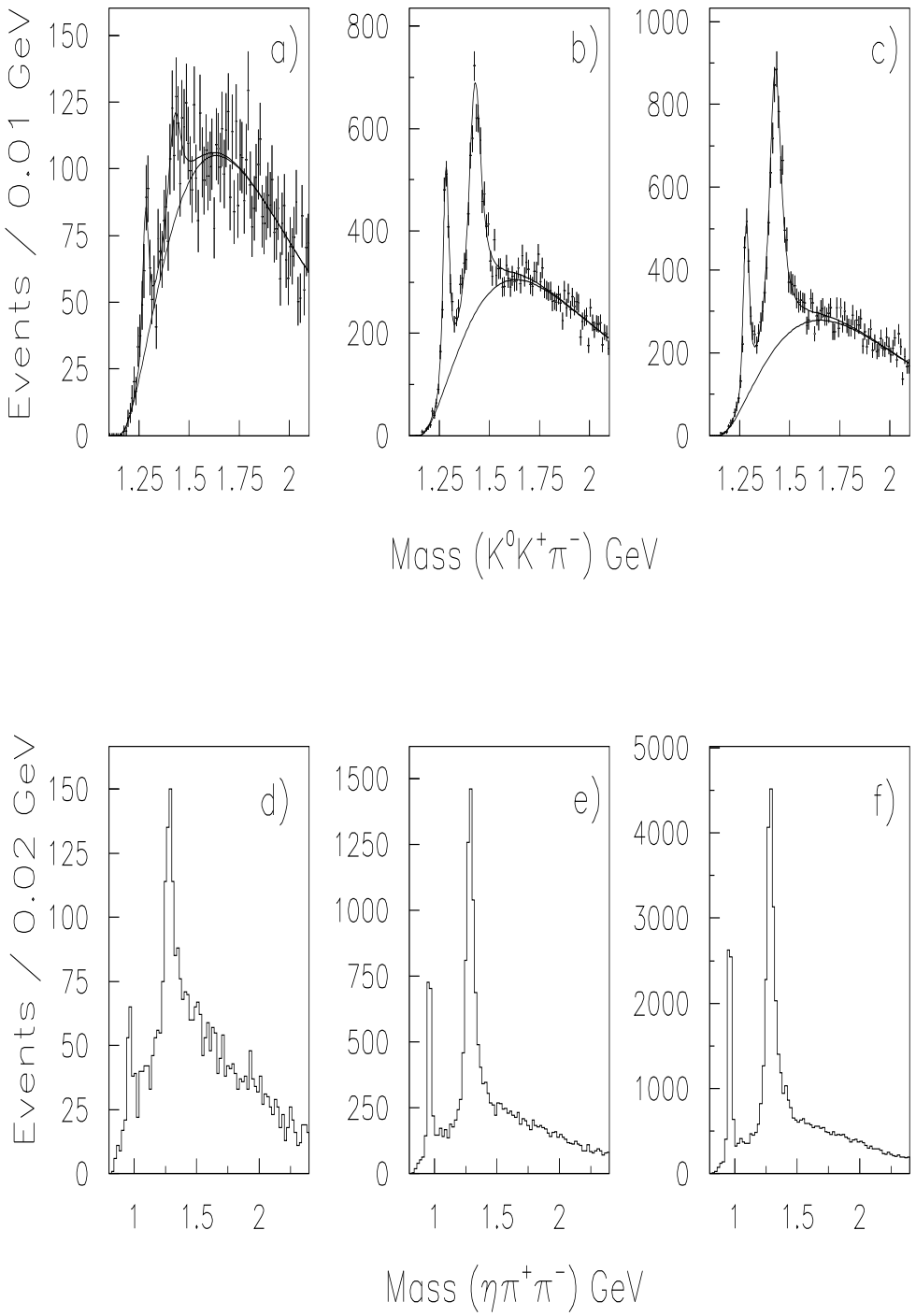

Figure 6: $K^0_S K^{\pm}\pi^{\mp}$ mass spectrum for a) $dP_T < 0.2$ GeV, b) $0.2 < dP_T < 0.5$ GeV and c) $dP_T > 0.5$ GeV and the $\eta\pi^+\pi^-$ mass spectrum for d) $dP_T < 0.2$ GeV, e) $0.2 < dP_T < 0.5$ GeV and f) $dP_T > 0.5$ GeV.

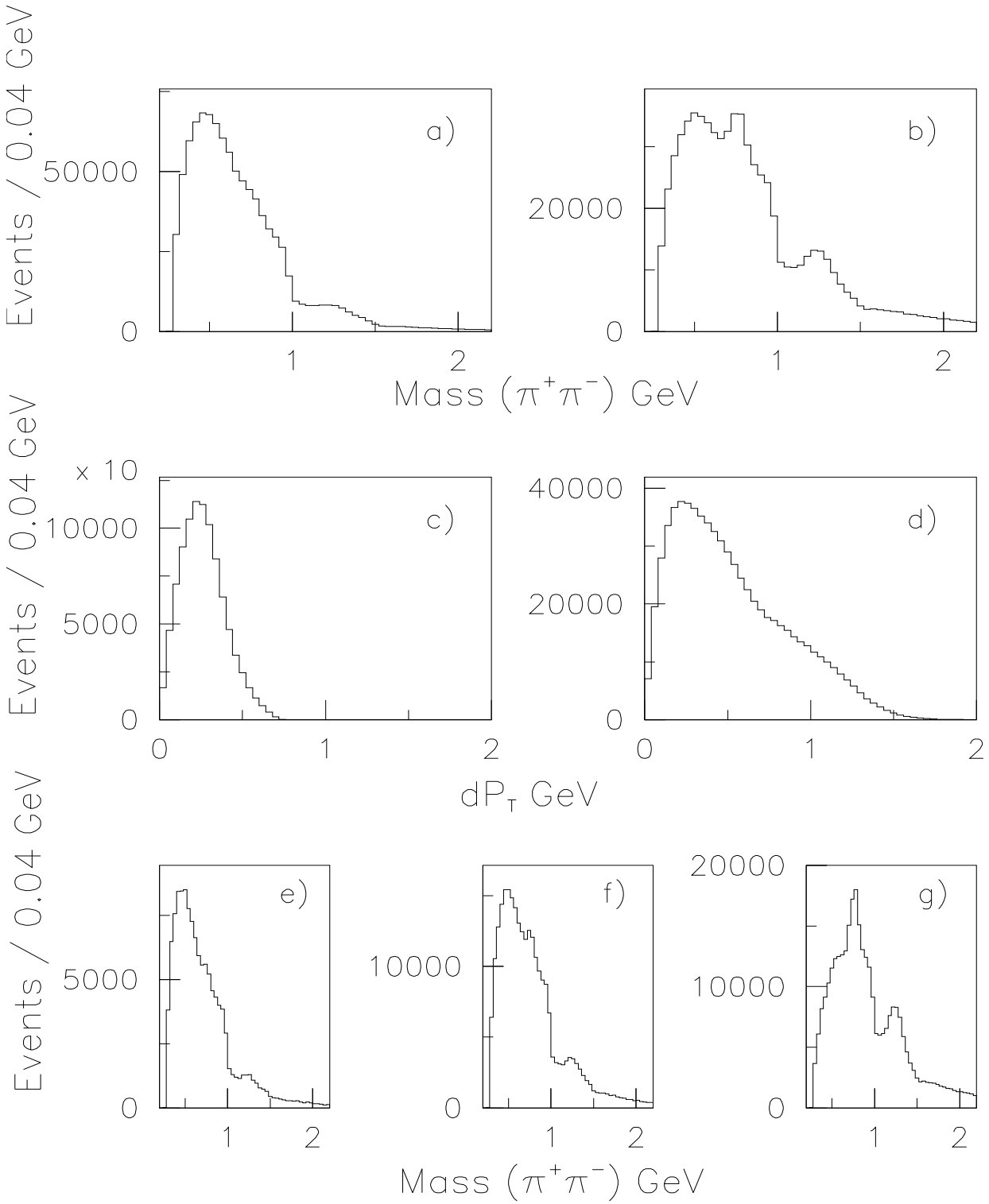

Figure 7: Results of cutting on the four momentum transferred at the proton vertices. The $\pi^+\pi^-$ mass spectrum for a) $|t_f| < 0.15$ and $|t_s| < 0.15$ GeV^2 and c) $|t_f| > 0.15$ and $|t_s| > 0.15$ GeV^2. The dP_T distribution for c) $|t_f| < 0.15$ and $|t_s| < 0.15$ GeV^2 and d) $|t_f| > 0.15$ and $|t_s| > 0.15$ GeV^2. The $\pi^+\pi^-$ mass spectrum for $|t_f| > 0.15$ and $|t_s| > 0.15$ GeV^2 and e) $dP_T < 0.2$ GeV, f) $0.2 < dP_T < 0.5$ GeV and g) $dP_T > 0.5$ GeV.

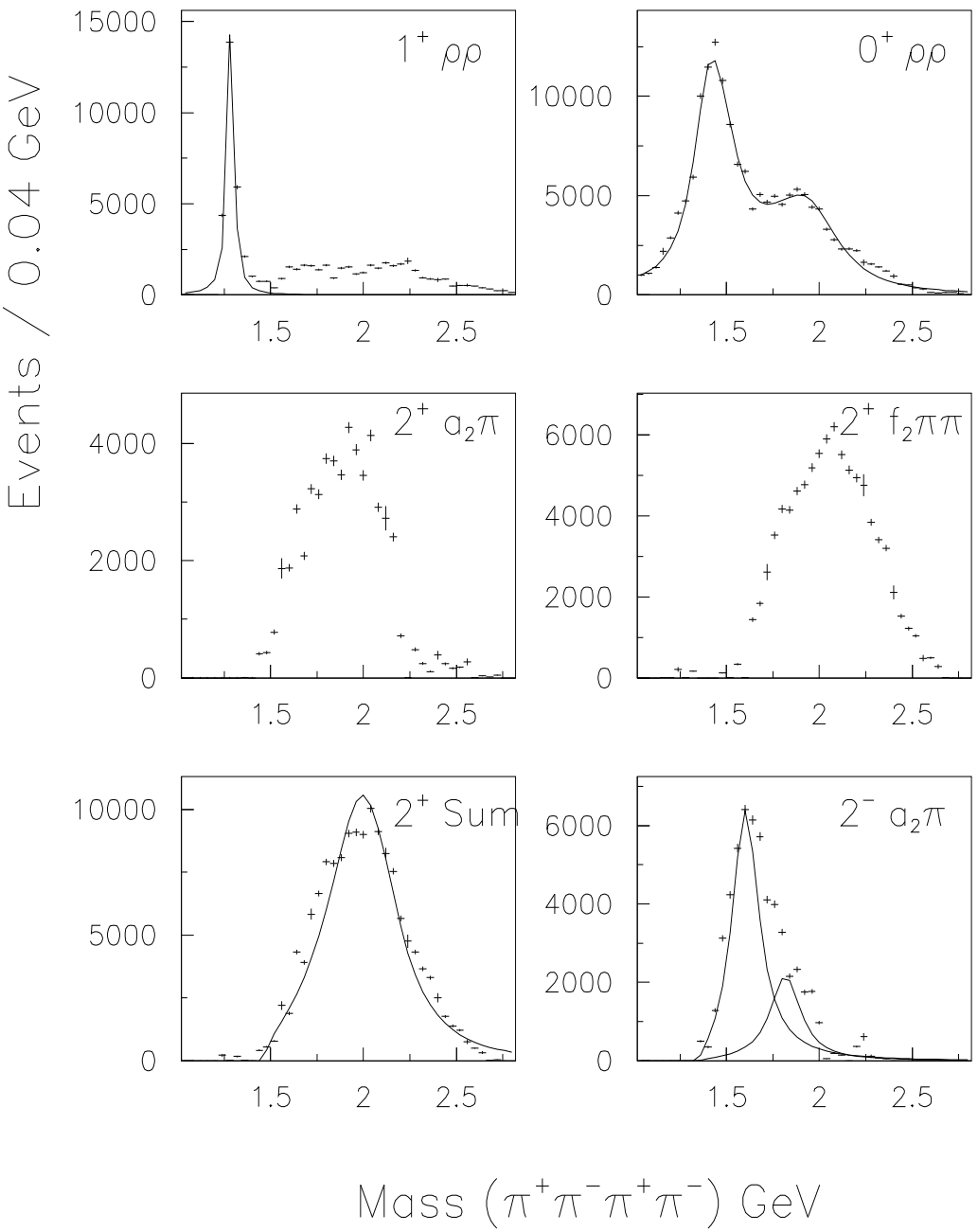

Figure 8: Results of the spin parity analysis of the $\pi^+\pi^-\pi^+\pi^-$ final state. The superimposed curves are the resonance contributions coming from the fits described in the text.

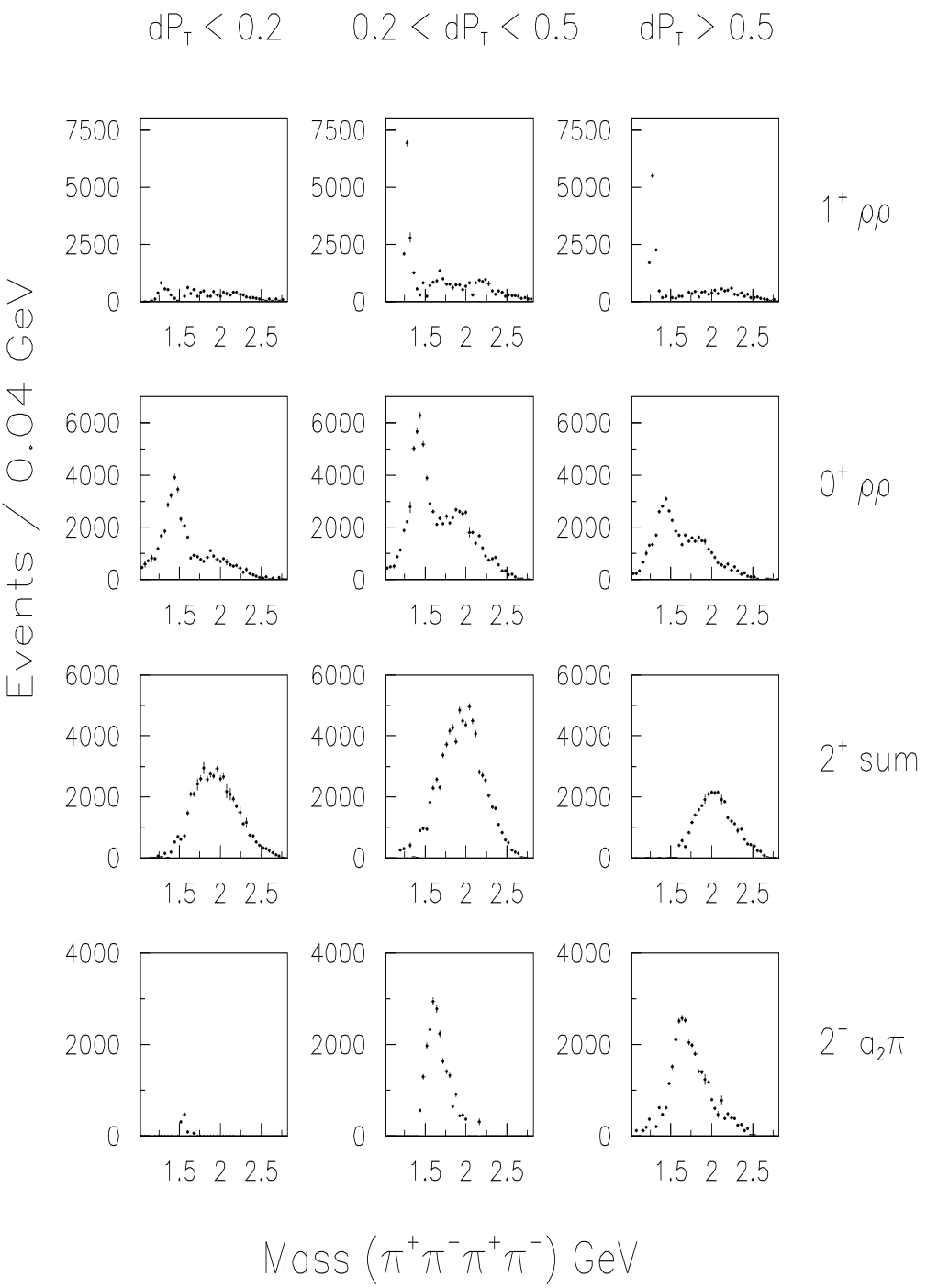

Figure 9: Results of the spin parity analysis of the $\pi^+\pi^-\pi^+\pi^-$ final state as a function of dP_T.

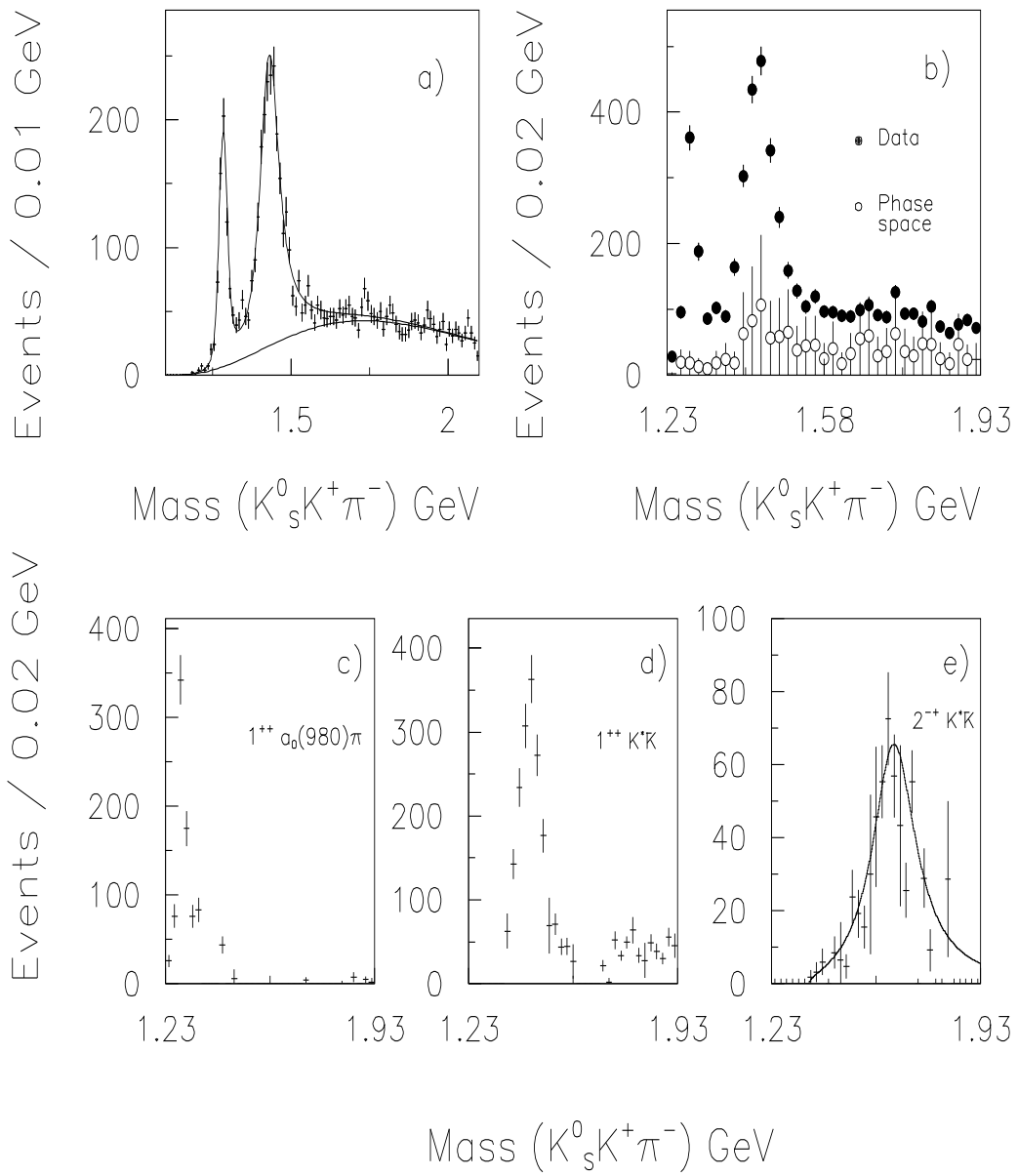

Figure 10: The $K^0_S K^\pm\pi^\mp$ data with the $K^\pm$ identified by the Čerenkov counter. a) Mass spectrum with fit described in the text, b) the $K^0_S K^\pm\pi^\mp$ mass spectrum used in the spin analysis and the resulting phase space contribution, c) the $J^{PG} = 1^{++}$ $a_0(980)\pi$ wave, d) the $J^{PG} = 1^{++}$ $K^*\overline{K}$ wave and e) the $J^{PG} = 2^{-+}$ $K^*\overline{K}$ wave.

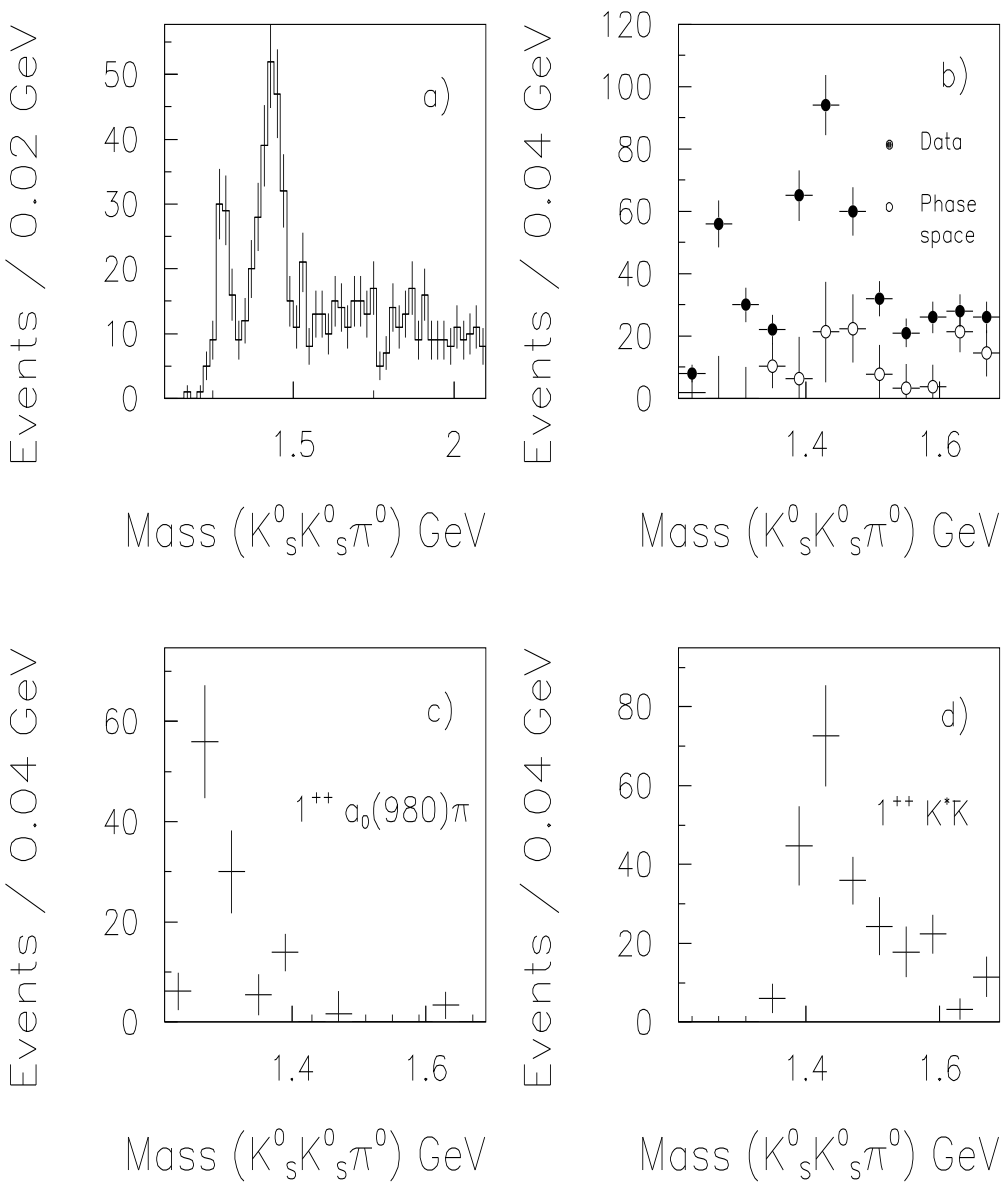

Figure 11: The $K^0_S K^0_S \pi^0$ sample. a) Mass spectrum, b) the $K^0_S K^0_S \pi^0$ mass spectrum used in the spin analysis and the resulting phase space contribution, c) the $J^{PC} = 1^{++}$ $a_0(980)\pi$ wave and d) the $J^{PC} = 1^{++}$ $K^*\overline{K}$ wave.

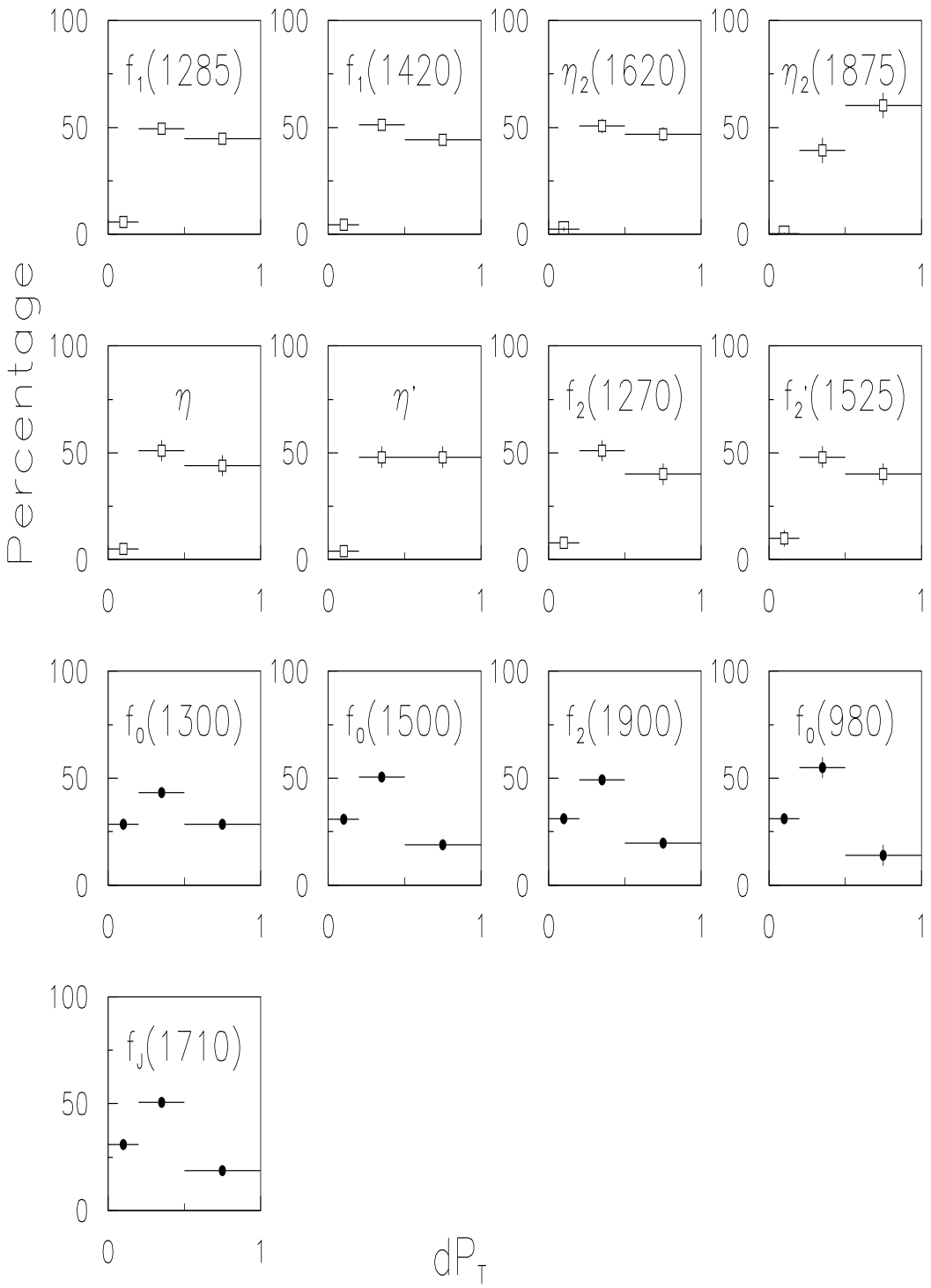

Figure 12: The percentage of the resonance as a function of dP_T

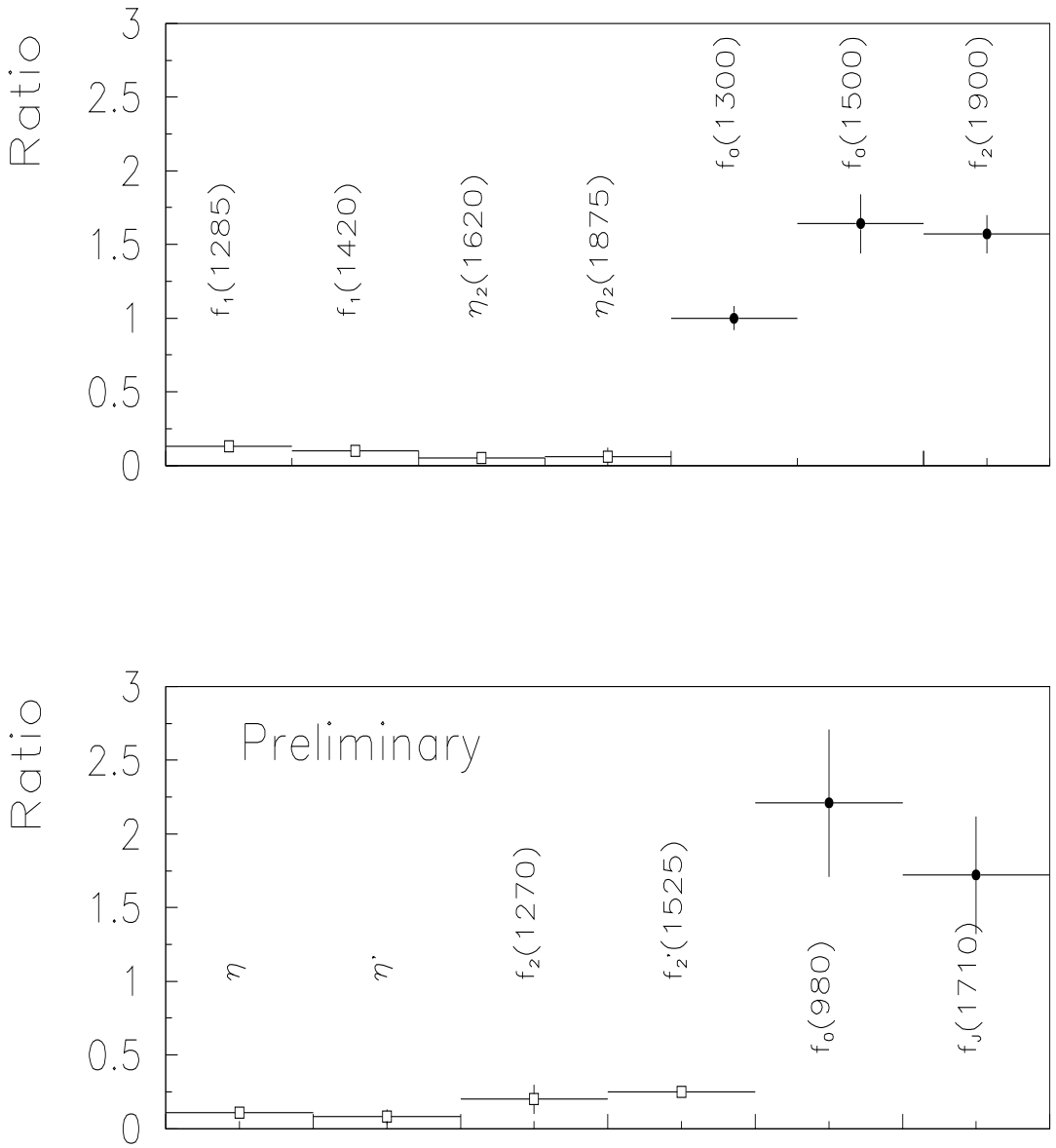

Figure 13: The ratio of the amount of resonance with $dP_T \leq 0.2$ to the amount with $dP_T \geq 0.5$ GeV.